nature neuroscience

The serine hydrolase ABHD6 controls the accumulation and efficacy of 2-AG at cannabinoid receptors

William R Marrs[1], Jacqueline L Blankman[2,11], Eric A Horne[3,11], Aurore Thomazeau[4], Yi Hsing Lin[3], Jonathan Coy[3], Agnes L Bodor[5], Giulio G Muccioli[6], Sherry Shu-Jung Hu[7], Grace Woodruff[8], Susan Fung[1], Mathieu Lafourcade[4], Jessica P Alexander[2], Jonathan Z Long[2], Weiwei Li[2], Cong Xu[3], Thomas Möller[9], Ken Mackie[7], Olivier J Manzoni[4], Benjamin F Cravatt[2] & Nephi Stella[3,10]

© 2010 Nature America, Inc. All rights reserved.

The endocannabinoid 2-arachidonoylglycerol (2-AG) regulates neurotransmission and neuroinflammation by activating CB_1 cannabinoid receptors on neurons and CB_2 cannabinoid receptors on microglia. Enzymes that hydrolyze 2-AG, such as monoacylglycerol lipase, regulate the accumulation and efficacy of 2-AG at cannabinoid receptors. We found that the recently described serine hydrolase α-β-hydrolase domain 6 (ABHD6) also controls the accumulation and efficacy of 2-AG at cannabinoid receptors. In cells from the BV-2 microglia cell line, ABHD6 knockdown reduced hydrolysis of 2-AG and increased the efficacy with which 2-AG can stimulate CB_2-mediated cell migration. ABHD6 was expressed by neurons in primary culture and its inhibition led to activity-dependent accumulation of 2-AG. In adult mouse cortex, ABHD6 was located postsynaptically and its selective inhibition allowed the induction of CB_1-dependent long-term depression by otherwise subthreshold stimulation. Our results indicate that ABHD6 is a rate-limiting step of 2-AG signaling and is therefore a bona fide member of the endocannabinoid signaling system.

In the nervous system, the endocannabinoids (eCBs) arachidonoylethanolamide (anandamide) and 2-AG are produced and inactivated by neurons and glia[1,2]. The production of eCBs increases in response to specific stimuli, including membrane receptor activation, ion channel opening and calcium influx[2]. eCBs are inactivated by cellular uptake followed by intracellular enzymatic hydrolysis[3,4]. The balance between this production and inactivation dictates the levels of extracellular eCB accumulation and the ensuing activation of CB_1 receptors expressed by neurons (regulating neurotransmitter release) and CB_2 receptors expressed by microglia (regulating their motility and ability to produce immunomodulators)[4–7]. Thus, the enzymatic steps that control the production and inactivation of eCBs constitute promising molecular targets for indirectly modulating CB_1 and CB_2 receptor activity, and thereby controlling neurotransmission and neuroinflammation.

Of all the steps that control the accumulation of eCBs, the hydrolytic enzymes that inactivate anandamide and 2-AG represent the most promising pharmacological and genetic targets for fine-tuning the local accumulation of these lipid transmitters. Inhibition of fatty acid amide hydrolase (FAAH) increases anandamide levels in the brain and leads to CB_1-mediated analgesia, and also has anxiolytic and antidepressant effects[8–10]. The inhibition of monoacylglycerol lipase (MAGL) increases 2-AG levels in the brain and leads to CB_1-mediated analgesia and hypomotility[11–13]. Notably, these therapeutic outcomes are achieved without eliciting the broad spectrum of cognitive effects that are typically associated with direct CB_1 receptor agonists[8–12]. Conversely, concomitant inhibition of FAAH and MAGL leads to an increase in the levels of both anandamide and 2-AG in the brain, recapitulating many of the effects produced by direct CB_1 receptor agonists[14]. Together, these results suggest that the selective inhibition of distinct eCB-hydrolyzing enzymes allows differential control of eCB signaling, with each hydrolase likely to provide unique therapeutic opportunities. This idea has led to the search for novel enzymes responsible for eCB hydrolysis.

There is evidence that, in addition to MAGL, the brain expresses other enzymes that can hydrolyze 2-AG. Pharmacological inhibition of MAGL in crude brain homogenates does not fully eliminate 2-AG hydrolysis, leaving ~20% of this activity intact[15,16]. Furthermore, immunoprecipitation of MAGL from brain cytosolic fractions reduces 2-AG hydrolysis by only ~50%[17]. BV-2 cells hydrolyze 2-AG even though they do not express *MAGL* mRNA[18]. Two new enzymes that are expressed in the brain and can hydrolyze 2-AG (ABHD6 and ABHD12) were recently identified using a functional proteomics approach[15] (activity-based protein profiling–multidimensional protein identification technology:

[1]Neurobiology and Behavior Graduate Program, University of Washington, Seattle, Washington, USA. [2]The Skaggs Institute for Chemical Biology and Department of Chemical Physiology, The Scripps Research Institute, La Jolla, California, USA. [3]Department of Pharmacology, University of Washington, Seattle, Washington, USA. [4]INSERM U862, Equipe Physiopathologie de la plasticité synaptique, Bordeaux, France. [5]Department of Otolaryngology, University of Washington, Seattle, Washington, USA. [6]Bioanalysis and Pharmacology of Bioactive Lipids Laboratory, CHAM7230, Louvain Drug Research Institute, Université catholique de Louvain, Bruxelles, Belgium. [7]Department of Psychological and Brain Sciences, Gill Center for Biomolecular Science, Indiana University, Bloomington, Indiana, USA. [8]Neurobiology Undergraduate Program, University of Washington, Seattle, Washington, USA. [9]Department of Neurology, University of Washington, Seattle, Washington, USA. [10]Department of Psychiatry and Behavioral Sciences, University of Washington, Seattle, Washington, USA. [11]These authors contributed equally to this work. Correspondence should be addressed to N.S. (nstella@uw.edu).

Received 16 March; accepted 23 June; published online 25 July 2010; doi:10.1038/nn.2601

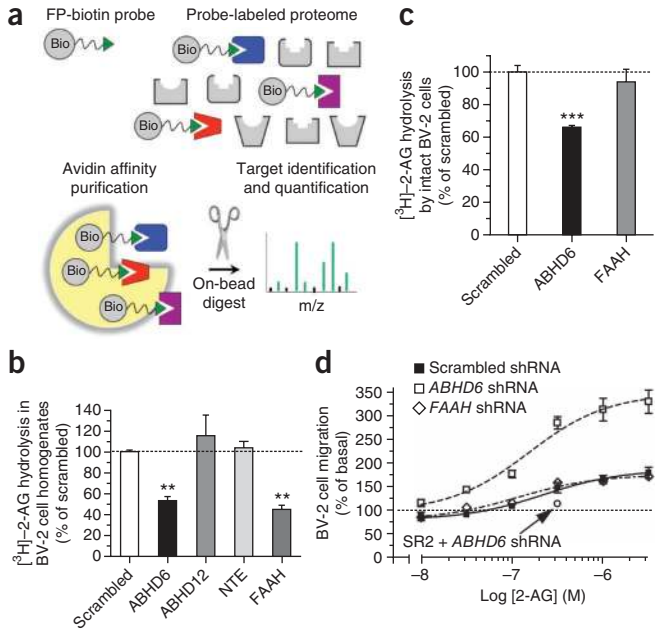

Figure 1 ABHD6 hydrolyzes 2-AG in BV-2 cells and controls the efficacy of 2-AG at CB_2 receptors. (**a**) Cartoon scheme of the ABPP-MudPIT procedure used to identify serine hydrolases expressed by BV-2 cells. (**b**) [^{3}H]–2-AG hydrolysis in homogenates prepared from BV-2 cells infected with shRNAs targeting *ABHD6*, *ABHD12*, *NTE* or *FAAH*, compared to scrambled shRNA. $^{**}P < 0.01$ compared to scrambled response (ANOVA one-way, Dunnett's post test). (**c**) [^{3}H]–2-AG hydrolysis in intact BV-2 cells infected with shRNA targeting either *ABHD6* or *FAAH*, compared to scrambled shRNA. $^{***}P < 0.0001$ compared to scrambled response (Student's *t* test). (**d**) 2-AG-induced cell migration of BV-2 cells infected with shRNA targeting *ABHD6* or *FAAH*, compared to scrambled shRNA. Data are expressed as percentage of basal migration (migration of the shRNA-treated clones in the presence of 0.1% DMSO). The 2-AG response is inhibited by pretreatment with the CB_2 receptor antagonist SR144528 (SR2, 200 nM). Data are shown as mean ± s.e.m. of 3–5 independent experiments, each performed in triplicate. The percentage knockdown was systematically verified for each infection and reported in **Supplementary Table 1**.

ABPP-MudPIT[19]). Whether these enzymes control the accumulation and efficacy of 2-AG at cannabinoid receptors in intact brain cells still needs to be directly tested. Here we used ABPP-MudPIT to identify the unknown 2-AG-hydrolyzing activity expressed by BV-2 cells, and found that it is ABHD6. We then tested whether ABHD6 controls the accumulation and efficacy of 2-AG at cannabinoid receptors in several models: intact BV-2 cells, mouse microglia in primary culture, mouse neurons in primary culture, and slices prepared from adult mouse brain.

RESULTS

ABHD6 hydrolyzes 2-AG in BV-2 cells

It has been shown that the unknown 2-AG-hydrolyzing activity expressed by BV-2 cells is sensitive to methyl arachidonyl fluorophosphonate (MAFP), a non-selective serine hydrolase inhibitor, and enriched in the mitochondrial fraction of these cells[18]. These results suggest that this enzyme can be isolated from BV-2 cell fractions by using a fluorophosphonate-based probe that targets serine hydrolases (FP-biotin)[20], and subsequently identified by the functional proteomics platform ABPP-MudPIT[19,21] (**Fig. 1a**). As an initial proof of concept, we found that the FP-biotin probe inhibited ~90% of the [^{3}H]-2-AG hydrolysis in BV-2 mitochondrial fractions (**Supplementary Fig. 1**). We carried out FP-biotin pull-down and subsequent ABPP-MudPIT analysis on both BV-2 mitochondrial and BV-2 cytosolic fractions (which show a ~10-fold difference in their amount of 2-AG-hydrolyzing activity[18]) with the goal of identifying serine hydrolases that are differentially expressed between these two fractions. Of the ten enzymes that were most highly enriched in the mitochondrial fraction (**Table 1**), four have been shown to hydrolyze 2-AG: ABHD12, NTE, FAAH and ABHD6 (ref. 15). MAGL was not detected in either of the BV-2 cell fractions, consistent with the previous finding that BV-2 cells do not express *MAGL* mRNA[18]. Thus, using FP-biotin probes and ABPP-MudPIT analysis, we identified ABHD12, NTE, FAAH and ABHD6 as viable candidates for the unknown 2-AG-hydrolyzing activity expressed by BV-2 cells.

We then used short hairpin RNA (shRNA) constructs to selectively knockdown the expression of each candidate enzyme in BV-2 cells to determine the relative contribution of each enzyme to the 2-AG hydrolysis measured in these cells. To obtain reliable knockdowns of each enzyme, we tested 25 shRNA constructs (**Supplementary Table 1**). Using the most efficient shRNAs, we found that knocking down the expression of *ABHD6* or *FAAH* each reduced [^{3}H]-2-AG hydrolysis in BV-2 cell homogenates by ~50%, whereas knocking down the expression of *ABHD12* or *NTE* had no significant effect (**Fig. 1b**). These data provide two important results. First, they confirm genetically that FAAH is responsible for ~50% of the [^{3}H]-2-AG hydrolysis measured in BV-2 cell homogenates (consistent with the finding that ~50% of the [^{3}H]-2-AG hydrolysis in BV-2 cell homogenates is sensitive to the FAAH inhibitor URB597[18]). Second, they suggest that ABHD6 (rather than ABHD12 or NTE) is responsible for the remaining 50% of the 2-AG hydrolysis in BV-2 cell homogenates, and thus lead us to conclude that ABHD6 is the novel enzyme for which we have been searching.

ABHD6 controls 2-AG's efficacy at CB_2 receptors

Results showing that an enzyme hydrolyzes a specific lipid in cell homogenates do not necessarily mean that the enzyme also hydrolyzes this lipid in intact cells. For example, FAAH hydrolyzes both anandamide and 2-AG in cell homogenates, but often only hydrolyzes anandamide in intact cells[18,22]. To determine whether ABHD6 hydrolyzes

Table 1 Four serine hydrolases were identified as candidates for the 2-AG–hydrolyzing activity measured in BV-2 cells

IPI number	Common name	Abbreviation	2-AG hydrolase activity	Spectral counts (mitochondrial fraction)	Spectral counts (cytosolic fraction)
IPI00331610	Patatin-like phospholipase domain 7 (NTE-related esterase)	PNPLA7	No	163	0
IPI00165731*	α-β hydrolase 12	ABHD12	Yes	44	0
IPI00128034*	Neuropathy target esterase	NTE	Yes	31	0
IPI00117176*	Fatty acid amide hydrolase	FAAH	Yes	24	0
IPI00321386*	α-β hydrolase 6	ABHD6	Yes	23	0
IPI00108883	FAM108B	FAM108B	No	23	0
IPI00403586	Arylacetamide deacetylase-like 1 (KIAA1363)	AADACL1	No	260	1
IPI00170213	α-β hydrolase 11	ABHD11	No	64	2
IPI00319188	Lipoprotein lipase	LPL	No	37	2
IPI00136683	Acyl coenzyme A thioester hydrolase 2	ACOT2	No	35	3

ABPP was performed on subcellular fractions from BV-2 cells to identify functional serine hydrolases. Listed are the ten enzymes that were the most abundant in the mitochondrial fraction relative to the cytosolic fraction.
*indicates enzymes that are known to hydrolyze 2-AG when transfected and their activity assessed in homogenates.

© 2010 Nature America, Inc. All rights reserved.

Table 2 ***ABHD6*** **is abundantly expressed in brain and more is found in neurons than microglia**

	HPRT CT	δCT (*ABHD6*)	Relative (%)
Brain	21.5–23.7	1.8	100
BV-2	22.9–23.2	3.9	23
Microglia	20.8–23.0	4.7	13
Neurons	23.2–24.2	3	44

Levels of *ABHD6* mRNA were quantified by qPCR and normalized to the housekeeping gene *HPRT*. Here the range of threshold cycles (CT) that we obtained in our measurements is provided, showing that *HPRT* can be used to compare *ABHD6* mRNA levels between different cells and tissue. Relative expression levels of *ABHD6* (calculated using δ-δCT) were assessed in BV-2 cells, microglia and neurons, and compared to total brain (which was set at 100%). Independent qPCR measurements were performed in independent cell cultures and brain tissue samples (N = 3 to 4).

2-AG in intact cells, we incubated intact BV-2 cells in culture with [^{3}H]-2-AG and measured the production of free [^{3}H]-glycerol. Intact BV-2 cells efficiently hydrolyzed [^{3}H]-2-AG, and this activity was significantly reduced in BV-2 cells infected with shRNA targeting *ABHD6*, whereas this activity was unaffected in BV-2 cells infected with shRNA targeting *FAAH* (**Fig. 1c**). These data show that, unlike FAAH, ABHD6 hydrolyzes 2-AG in intact BV-2 cells.

BV-2 cell migration is stimulated by 2-AG, and this response is blocked by the CB_2 receptor antagonist SR144528 (ref. 23). Here, to determine whether ABHD6 controls the efficacy of 2-AG at cannabinoid receptors, we tested whether *ABHD6* knockdown in BV-2 cells increases this response. Using an unbiased method that quantifies cell migration with a near-infrared-emitting dye[24], we found that 2-AG increased the migration of BV-2 cells infected with either scrambled shRNA or shRNA targeting *FAAH* ~2-fold, but stimulated by ~3-fold the migration of BV-2 cells infected with shRNA targeting *ABHD6* (**Fig. 1d**). This result supports the notion that less 2-AG is hydrolyzed when ABHD6 is knocked down, and thus more 2-AG reaches and activates CB_2 receptors. Three controls are worth noting here. First, the stimulatory effect of 2-AG on the migration of *ABHD6*-knockdown BV-2 cells was blocked by the CB_2 receptor antagonist SR144528 (**Fig. 1d**). Second, CB_2 receptor expression (as determined by radioligand binding using [^{3}H]-CP55940 and SR144528 at 100 nM) did not differ between BV-2 cells infected with scrambled shRNA or shRNA targeting *ABHD6* (data not shown), indicating that these infections did not affect CB_2 receptor expression. Third, the half-maximum effective concentration (EC50) of 2-AG to stimulate BV-2 cell migration did not differ between BV-2 cells infected with scrambled shRNA or shRNA targeting *ABHD6*, suggesting that the coupling of CB_2 receptors to second messenger signaling was not affected by shRNA treatment (**Fig. 1d**). Together, these results indicate that ABHD6 hydrolyzes 2-AG in intact cells and controls its efficacy at CB receptors, making this enzyme a rate-limiting step in controlling the bioactivity of this lipid transmitter.

Neurons express ABHD6

To explore the expression of ABHD6 in primary brain cells, we quantified both *ABHD6* mRNA and ABHD6 enzymatic activity in various mouse brain preparations. Using quantitative PCR (qPCR), we found that *ABHD6* mRNA was abundant in adult mouse brain and neurons in primary culture, and low in mouse microglia in primary culture (**Table 2**). To measure the enzymatic activity of ABHD6, we determined the amount of [^{3}H]-2-AG hydrolysis that is blocked by WWL70, a highly selective ABHD6 inhibitor[25]. This study provided three further pieces of evidence that WWL70 is an effective and specific inhibitor of mouse ABHD6 activity. First, WWL70 dose-dependently inhibited [^{3}H]-2-AG hydrolysis in homogenates prepared from *ABHD6*-transfected COS-7 cells (**Fig. 2a**); by contrast, the selective MAGL inhibitor JZL184[11] had no significant effect on [^{3}H]-2-AG hydrolysis in these homogenates (**Fig. 2b**). Second, WWL70 inhibited ~50% of the [^{3}H]-2-AG hydrolysis in BV-2 cell homogenates (**Fig. 2c**). Third, WWL70 did not directly interact with CB_1 or CB_2 receptors (**Supplementary Fig. 2**).

WWL70 inhibited ~20% of the [^{3}H]-2-AG hydrolysis in homogenates prepared from adult mouse brain (data not shown), which is in line with a previous report showing that ABHD6 accounts for a small portion of the overall 2-AG hydrolysis measured in whole brain homogenates[15]. In homogenates prepared from neurons in primary culture, WWL70 inhibited ~50% of the total [^{3}H]-2-AG hydrolysis (**Fig. 2d**). These results reveal that whereas adult mouse brain shows a higher overall 2-AG hydrolysis activity than neurons in primary culture (13.2 versus 3.8 pmol of 2-AG per mg of protein per min), the relative contribution of ABHD6 is greater in neurons in primary culture than in adult mouse brain. In homogenates prepared from microglia in primary culture, WWL70 had no significant effect on [^{3}H]-2-AG hydrolysis (**Supplementary Fig. 3**), consistent with the lower level of *ABHD6* mRNA in these cells. Thus, we focused our next set of experiments on the functional significance of ABHD6 in neurons.

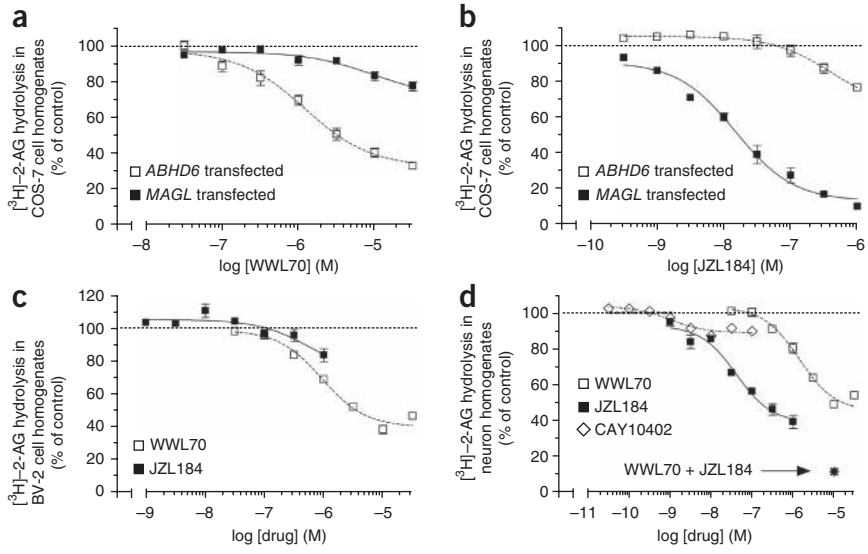

Figure 2 Effect of the ABHD6 inhibitor WWL70 and the MAGL inhibitor JZL184 on [^{3}H]–2-AG hydrolysis in cell homogenates. [^{3}H]–2-AG hydrolysis in homogenates prepared from (**a**,**b**) COS-7 cells transfected with mouse *ABHD6* (5 μg of protein per reaction) or with mouse *MAGL* (0.25 μg of protein per reaction); (**c**) BV-2 cells (10 μg of protein per reaction); and (**d**) mouse neurons in primary culture (1 μg of protein per reaction). For the combination of the two inhibitors in **d**, WWL70 was used at 10 μM and JZL184 at 1 μM. Data are mean ± s.e.m. of 3 to 4 independent experiments. Each experiment was performed in triplicate with homogenates or cells from independent transfections and cell preparations. Transfection of COS-7 cells with *ABHD6* increased [^{3}H]–2-AG hydrolysis by about twofold compared to COS-7 cells transfected with empty vector, whereas transfection of COS-7 cells with *MAGL* increased [^{3}H]–2-AG hydrolysis by 17-fold compared to COS-7 cells transfected with empty vector (data not shown).

© 2010 Nature America, Inc. All rights reserved.

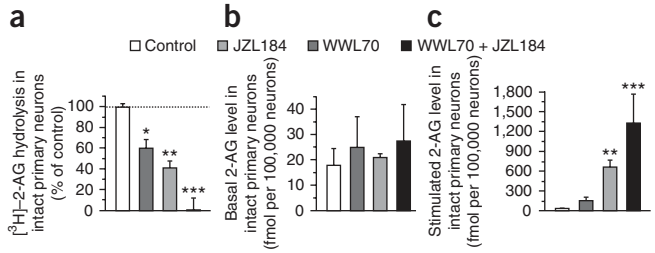

Figure 3 Effect of WWL70 and JZL184 on [^{3}H]–2-AG hydrolysis and 2-AG accumulation in intact neurons in primary culture. (**a**) [^{3}H]–2-AG hydrolysis by intact primary neurons after 30 min pretreatment with WWL70 (10 μM) or JZL184 (1 μM). The data are expressed as % of control hydrolysis (pretreatment with 0.1% DMSO). (**b**,**c**) Levels of 2-AG in intact primary neurons pretreated for 30 min with WWL70 (10 μM), JZL184 (1 μM) or vehicle (0.1% DMSO, control; **b**) and stimulated with glutamate (100 μM) and carbachol (1 mM) for 2.5 min, after which lipids were extracted and 2-AG amounts measured by GC-MS (**c**). Treatment with glutamate plus carbachol led to a 2.5-fold increase in 2-AG amounts (in fmol per 100,000 cells: 18 to 44). Data are shown as mean ± s.e.m. of 3–6 independent experiments. Experiments were performed in triplicate for the hydrolysis assay and in duplicate for 2-AG quantification by GC-MS, using cells from independent cell culture preparations. *$P < 0.05$, **$P < 0.01$, ***$P < 0.001$ (ANOVA one-way, Bonferroni's post test).

ABHD6 and MAGL control 2-AG accumulation in neurons

Previous results indicate that 2-AG hydrolysis in neurons is mediated by MAGL[26], and we now show that ABHD6 is also likely to be involved. We investigated the relative contributions of MAGL and ABHD6 to 2-AG hydrolysis in two neuronal preparations: (i) Homogenates prepared from neurons in primary culture, and (ii) intact neurons in primary culture. We used the ABHD6 inhibitor WWL70 and the MAGL inhibitor JZL184. We confirmed the efficacy of JZL184 at inhibiting mouse MAGL activity, as it inhibited [^{3}H]-2-AG hydrolysis in homogenates prepared from *MAGL*-transfected COS-7 cells (**Fig. 2b**). Note that these inhibitors can be used to discriminate the activities of these two enzymes, as 1 μM JZL184 did not significantly affect 2-AG hydrolysis in homogenates prepared from *ABHD6*-transfected COS-7 cells and 10 μM WWL70 did not significantly affect 2-AG hydrolysis in homogenates prepared from *MAGL*-transfected COS-7 cells (**Fig. 2a**,**b**). When tested in homogenates prepared from primary neurons, JZL184 inhibited ~50% of the total 2-AG hydrolysis (**Fig. 2d**). Furthermore, the combination of the maximally effective concentrations of WWL70 and JZL184 blocked almost all of the 2-AG hydrolysis in these homogenates (**Fig. 2d**). These results show that ABHD6 and MAGL are each responsible for about half of the total 2-AG hydrolysis in primary neuron homogenates. The remaining 2-AG hydrolysis in neuron homogenates (~10%) is probably mediated by FAAH, as its selective inhibitor CAY10402 blocks 10% of this activity (**Fig. 2d**).

We then tested the relative contributions of ABHD6 and MAGL to 2-AG hydrolysis in intact neurons. Here we performed two sets of experiments. First, we incubated intact neurons in primary culture with [^{3}H]-2-AG and measured the production of [^{3}H]-glycerol. These cells efficiently hydrolyzed [^{3}H]-2-AG and this activity was significantly reduced by treatment with either WWL70 or JZL184, with JZL184 being more efficacious (**Fig. 3a**). The combination of WWL70 and JZL184 (10 and 1 μM, respectively) blocked all of the 2-AG hydrolysis in these cells (**Fig. 3a**), which supports the idea that FAAH does not hydrolyze 2-AG in intact cells. In the second set of experiments, we pretreated neurons in primary culture with WWL70 and JZL184 (alone and in combination), and then quantified eCB levels under either basal or stimulated conditions by using gas chromatography-mass spectrometry (GC-MS). The stimulation we chose was a combination of glutamate and carbachol because this treatment has been shown to increase 2-AG production in these cells[27]. Neither WWL70 nor JZL184 affected basal 2-AG levels (**Fig. 3b**). Conversely, WWL70 induced a ~2-fold potentiation of the stimulated response, and JZL184 induced a ~7-fold potentiation of the stimulated response (**Fig. 3c**). Combining the two inhibitors resulted in a more significant potentiation of the stimulated response than JZL184 alone (**Fig. 3c**), recapitulating what was seen with our intact cell hydrolysis assay (**Fig. 3a**). Neither of these inhibitors had a significant effect on anandamide levels (**Supplementary Fig. 4**). These results show that both ABHD6 and MAGL regulate stimulus-dependent accumulation of 2-AG without affecting the basal level of this eCB in neurons in primary culture. Although it is clear that MAGL is much more efficient at controlling the stimulated accumulation of 2-AG in these cells, it seems that ABHD6 and MAGL might have non-overlapping functions. Specifically, WWL70 increased by ~2-fold the stimulated accumulation of 2-AG in both the presence and absence of JZL184 (**Supplementary Fig. 5**). This suggests that ABHD6 and MAGL independently control the stimulated accumulation of 2-AG in intact neurons.

ABHD6 regulates eCB-LTD in adult mouse prefrontal cortex

Both CB_1 receptors and MAGL are expressed presynaptically in neurons[28]. To visualize ABHD6 expression, we generated a rabbit polyclonal antibody that recognizes a 38-amino-acid sequence in the middle of the mouse ABHD6 protein (**Supplementary Fig. 6**). This antibody recognizes ABHD6, as it labels *ABHD6*-transfected COS-7 cells (using *GFP* as a

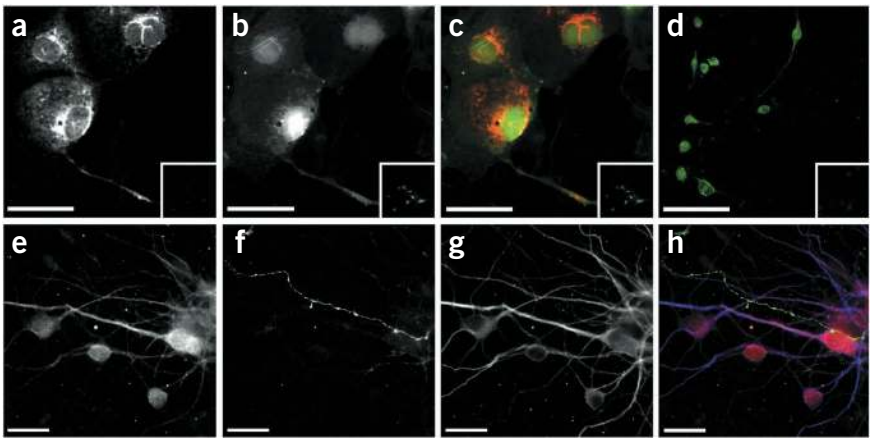

Figure 4 Visualization of ABHD6 protein in different cell types. (**a**–**h**) Representative images of COS-7 cells transfected with plasmids encoding *ABHD6* and *GFP* (**a**–**c**; scale bar, 50 μm), BV-2 cells (**d**; scale bar, 100 μm) and mouse neurons in primary culture (**e**–**h**; scale bar, 20 μm). Fluorescence detection of primary antibodies recognizing ABHD6 (**a**, **d**, **e**; red in **c**, **h**), CB_1 receptor (**f**, green in **h**), or MAP2 (**g**, blue in **h**). Fluorescence detection of GFP (**b**, green in **c**). Insets show pre-incubation with 5 μg per ml of the ABHD6 immunizing peptide (**a**–**d**).

© 2010 Nature America, Inc. All rights reserved.

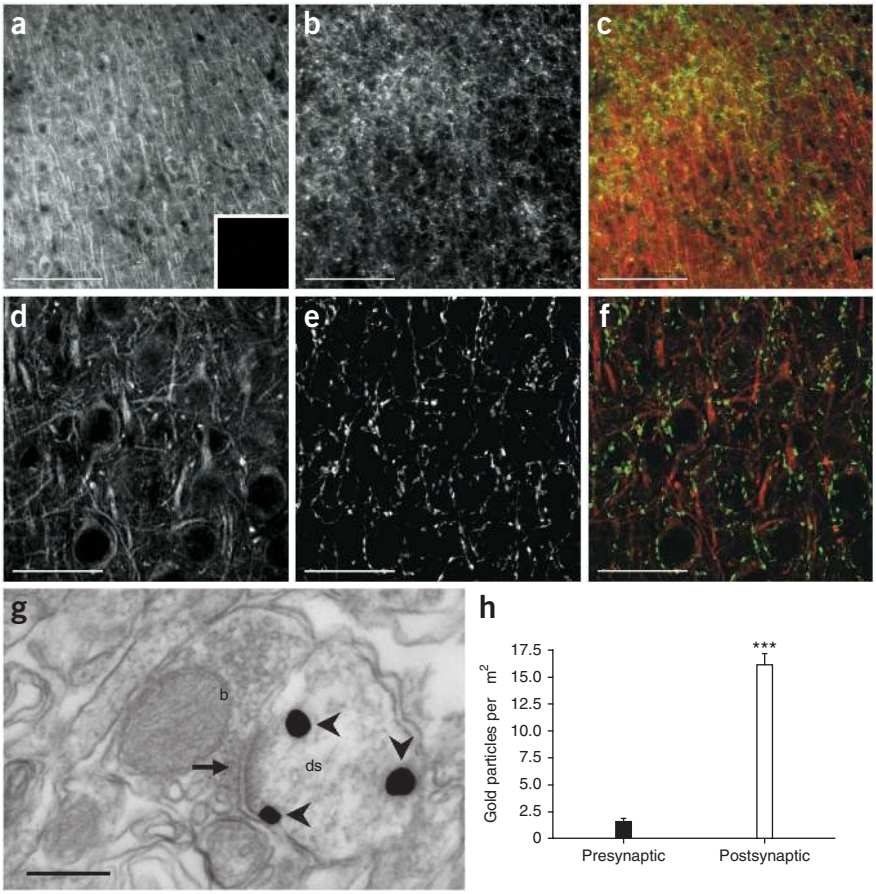

Figure 5 Localization of ABHD6 protein in mouse prefrontal cortex. (**a**–**f**) Fluorescent immunohistochemical staining of adult mouse prefrontal cortex (scale bars: **a**–**c**, 100 μm; **d**–**f**, 20 μm) using antibodies that recognize ABHD6 (**a**,**d**; red in **c**,**f**) and CB_1 receptors (**b**,**e**; green in **c**,**f**). Inset in **a** shows pre-incubation with 5 μg per ml of the ABHD6 immunizing peptide. (**g**) Electron micrograph of antibodies recognizing ABHD6 (arrowheads) in adult mouse prefrontal cortex, labeled with silver-enhanced gold particles (scale bar, 200 nm). Note that ABHD6 is predominantly found on the postsynaptic side of the synapse (arrow) in dendritic spines (ds), and not in presynaptic boutons (b). (**h**) Quantitative analysis of all electron microscopy images using ImageJ software. The number of gold particles on pre- and postsynaptic sides of identifiable synapses were manually counted and then normalized to the area of the respective structures for comparison. Data are mean ± s.e.m. of 154 identifiable synapses, in two animals. $^{***}P < 0.001$ (unpaired two-tailed *t*-test).

transfection marker; **Fig. 4a–c** and **Supplementary Fig. 7**), whereas it does not label *ABHD6*-transfected COS-7 cells when the antibody is pre-absorbed with the immunizing peptide (**Fig. 4a–c**) or when the antibody is tested on *pcDNA*-transfected COS-7 cells (**Supplementary Fig. 7**). Using this antibody, we confirmed ABHD6 expression in BV-2 cells (**Fig. 4d**) and a lack of detectable ABHD6 expression in primary microglia (data not shown). In neurons in primary culture, this antibody showed that ABHD6 is mainly expressed in the cell soma and dendrites, where it co-localizes with MAP2 and not with axonal CB_1 receptors (**Fig. 4e–h**). In adult mouse brain, ABHD6 is abundantly expressed in cortical areas (**Supplementary Fig. 8**). More specifically, in the prefrontal cortex, ABHD6 often juxtaposes, but does not overlap, with presynaptic CB_1 receptors (**Fig. 5a–f**). Accordingly, using electron microscopy, we found that most of the ABHD6 immunoreactivity was detected in postsynaptic structures (**Fig. 5g,h**). Using various cellular markers, we confirmed that ABHD6 is expressed by many principal glutamatergic neurons, as well as by some GABAergic interneurons and astrocytes, but not by microglia (**Supplementary Fig. 9**). Together, these results show that neurons express ABHD6, and that this enzyme is prevalent in the postsynaptic spines of glutamatergic neurons. This finding raises the question of whether ABHD6 participates in the control of 2-AG's efficacy at neuronal CB_1 receptors in the adult brain.

By activating presynaptic CB_1 receptors, 2-AG induces several forms of synaptic plasticity[29–31]. To test whether ABHD6 controls 2-AG's ability to induce synaptic plasticity, we tested long-term depression (LTD) in prefrontal cortical slices prepared from adult mouse. Sub-threshold stimulation of pyramidal neurons in layer 2 of this brain area induces eCB-dependent LTD (eCB-LTD) in layer 5 when a non-specific inhibitor of 2-AG hydrolysis, URB602, is added[32]. Importantly, the FAAH inhibitor URB597 has no effect on this response[32]. Thus, we sought to determine which 2-AG hydrolase(s), MAGL or ABHD6, is responsible for regulating this cortical eCB-LTD. First, we confirmed that sub-threshold stimulation (5 min at 10 Hz) in layer 2 does not induce LTD in layer 5 (**Fig. 6a**). Using this sub-threshold stimulation protocol, we found that application of WWL70 allowed the induction of robust LTD (a 22% reduction in synaptic transmission for at least 40 min after the stimulation). This response was mediated by CB_1 receptors, as it was fully blocked by the CB_1 antagonist AM251 (**Fig. 6b**). The MAGL inhibitor JZL184 also facilitated LTD induction at these

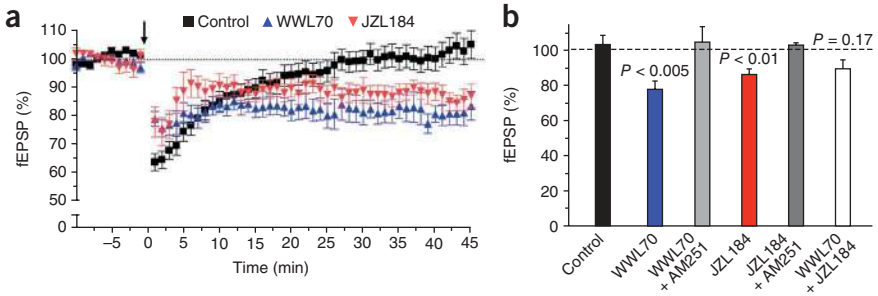

Figure 6 Effect of WWL70 and JZL184 on CB_1-dependent LTD in mouse prefrontal cortex. Field potentials measured in layer 5 after stimulation in layer 2 (arrow, 5 min at 10 Hz). Both the area and amplitude of the field excitatory postsynaptic potential (fEPSP) were measured (graphs depict area). Slices were preincubated for 10 min with WWL70 (10 μM), JZL184 (1 μM) or vehicle (0.01% DMSO, control), and the inhibitors remained present in the superfusion medium throughout the experiment. (**a**) Time course and (**b**) summary of the 40-min time point. Data are mean ± s.e.m. of at least ten different brain slices. Statistical significance (above bars) was calculated relative to control (Mann Whitney).

© 2010 Nature America, Inc. All rights reserved.

synapses (14%), and this response was also CB_1-dependent (**Fig. 6b**). Surprisingly, the combination of WWL70 and JZL184 in this paradigm did not induce significant LTD, which might reflect an increase in the baseline level (before electrical stimulation) of 2-AG in these brain slices after pre-treatment with both inhibitors. Together, these results indicate that, like MAGL, ABHD6 is a rate-limiting enzyme for 2-AG inactivation in adult mouse brain, and that its postsynaptic expression allows it to regulate the efficacy of 2-AG at presynaptic CB_1 receptors.

To further characterize the roles of ABHD6 and MAGL in regulating synaptic plasticity in cortex, we used two relevant short-term synaptic plasticity paradigms, namely depolarization-induced suppression of inhibition (DSI) and depolarization-induced suppression of excitation (DSE). Using standardized induction protocols, we found that neither DSI nor DSE could be induced in cortical layer 5 (**Supplementary Fig. 10**). In contrast, we could induce DSI in cortical layer 2; however, the decay rate of this effect was not altered by treatment with either WWL70 or JZL184 (**Supplementary Fig. 10**), suggesting that ABHD6 and MAGL are not involved in the regulation of this form of short-term synaptic plasticity in cortical layer 2.

DISCUSSION

BV-2 cells do not express *MAGL* and yet they efficiently hydrolyze 2-AG, providing evidence for the existence of another enzyme that can hydrolyze this eCB[18]. The serine hydrolases ABHD6 and ABHD12, which were identified in adult mouse brain, can hydrolyze 2-AG when they are heterologously expressed in COS-7 cells and their activity is assayed in cell homogenates[15]. We now report that ABHD6 is responsible for the previously uncharacterized endogenous 2-AG-hydrolyzing activity in BV-2 cells, and that this enzyme controls the accumulation and efficacy of 2-AG at cannabinoid receptors in intact BV-2 cells, neurons, and adult mouse brain slices, but not in primary microglia.

Although BV-2 cells are widely used as a surrogate model for studying the immune function of microglia, many laboratories have reported that their phenotype is quite different from that of microglia in primary culture and adult brain. Adding to this list of differences, we found that BV-2 cells express functional ABHD6, whereas microglia, whether they are in primary culture or in adult mouse brain, do not. It is worth noting that the phenotype of microglia is extremely plastic, and thus it is possible that specific pathogens or immunomodulators might induce ABHD6 expression in these cells. In line with this notion, Epstein-Barr virus antigens induce ABHD6 expression in B cells[33]. A question that remains unanswered at this point is: What is the enzyme responsible for the 2-AG-hydrolyzing activity measured in homogenates prepared from primary microglia, as this activity is unaffected by the ABHD6 inhibitor WWL70 and the MAGL inhibitor JZL184 (**Supplementary Fig. 3**)?

In neurons in primary culture, 2-AG hydrolysis is mediated by both MAGL and ABHD6; however, when assessing their relative contributions to this process, we found slight differences depending on the assay that was used and the conditions that were tested. Specifically, when measuring 2-AG hydrolysis in neuron homogenates, we found that ABHD6 and MAGL contributed about equally (**Fig. 2d**). Here, in a homogenous environment, the relative contributions of ABHD6 and MAGL to the hydrolysis of 2-AG are dictated by both their intrinsic enzymatic activity and their expression. Because ABHD6 has a lower intrinsic 2-AG hydrolysis activity than MAGL[15], our results suggest that ABHD6 is expressed at a higher level than MAGL in primary neurons. When determining the relative contributions of ABHD6 and MAGL to 2-AG hydrolysis in intact neurons in primary culture, we found that the less abundant enzyme, MAGL, has a greater role in controlling 2-AG levels than the more abundant enzyme, ABHD6 (**Fig. 3**). This predominant role for MAGL over ABHD6 in intact neurons in primary culture was found in two different experimental conditions: when [^{3}H]-2-AG was provided from the extracellular space, and when endogenous 2-AG production was stimulated by receptors expressed at the plasma membrane (glutamatergic and cholinergic receptors). These results indicate that MAGL and ABHD6 are found in distinct sub-cellular locations, and that MAGL is strategically positioned within intact neurons in primary culture to hydrolyze 2-AG when this lipid reaches the cells from the extracellular space, as well as when it is endogenously produced.

Three independent sets of data further support the notion that MAGL and ABHD6 have distinct sub-cellular locations in neurons, resulting in the independent control of 2-AG accumulation. First, dual inhibition of MAGL and ABHD6 activities in intact neurons in primary culture had an additive effect on both the hydrolysis of exogenously applied 2-AG and the stimulated production of endogenous 2-AG (**Fig. 3**). Second, an analysis of their amino acid sequences indicates that ABHD6 is likely to be an integral membrane enzyme, whereas MAGL is a cytosolic enzyme that peripherally associates with membranes[15,34]. Western blot analysis of sub-cellular fractions from mouse brain supports this prediction, as ABHD6 immunoreactivity was found only in the membrane fraction, whereas MAGL immunoreactivity was distributed between both membrane and cytosolic fractions (**Supplementary Fig. 11**). Third, our immunofluorescence and electron microscopy images revealed that ABHD6 is expressed in postsynaptic dendrites in the adult brain, whereas there is evidence that MAGL is localized to presynaptic axon terminals[28]. Thus, the relative contributions of MAGL and ABHD6 to the control of 2-AG levels in intact neurons in primary culture and adult brain are probably dictated by their distinct sub-cellular localizations.

Inhibition of either ABHD6 or MAGL had a similar effect on synaptic plasticity at cortical layer 5 excitatory synapses (that is, inhibition of either enzyme allowed the induction of CB1-dependent LTD by an otherwise sub-threshold stimulation; **Fig. 6**). This suggests that the amount of 2-AG that reaches presynaptic CB_1 receptors is controlled both at the site of 2-AG production (postsynaptic) by ABHD6 and at the site of the CB_1 receptor targets (presynaptic) by MAGL. This sort of redundancy is likely to offer the system greater versatility to fine-tune the magnitude and duration of 2-AG signaling. Furthermore, 2-AG produced by other cell types found in the nervous system, such as glia and invading immune cells, is also likely to be regulated at the source of production by these cells' own 2-AG–hydrolyzing enzyme(s)[35,36]. Thus, whereas ABHD6 is strategically positioned to regulate neuronal—and perhaps also astroglial—production of 2-AG, MAGL is well positioned to control the amount of 2-AG that reaches presynaptic CB_1 receptors regardless of the source of the 2-AG. We were surprised to find that the co-inhibition of both MAGL and ABHD6 did not allow subthreshold stimulation to produce significant LTD of cortical layer 5 glutamatergic synapses (**Fig. 6b**). Although it is counterintuitive, this result could reflect a saturation effect in which basal 2-AG levels in the brain slice are elevated by the inhibitors before the electrical stimulation, thus inducing LTD prematurely and reducing the measured difference between synaptic efficacy before and after the electrical stimulation. Accordingly, basal neuronal activity is much higher in brain slices than in dissociated neurons in primary culture, and thus inhibition of 2-AG hydrolysis would be expected to have a greater effect on basal 2-AG levels in brain slices (**Fig. 6**) than in neurons in primary culture (**Fig. 3**). Together, our results suggest that the relative contributions of MAGL, ABHD6 and any other 2-AG-hydrolyzing enzymes to the regulation

© 2010 Nature America, Inc. All rights reserved.

of 2-AG signaling will vary depending on the cellular origin of this eCB and the type of stimulation that increases its production. This arrangement could offer an additional modality in the control of 2-AG signaling in various pathophysiological conditions.

The identification and characterization of enzymes that hydrolyze eCBs is necessary to obtain a mechanistic understanding of this signaling system and to exploit these pathways for therapeutic gain. The criteria that a hydrolytic enzyme needs to fulfill to be considered a bona fide member of the eCB signaling system include showing that it hydrolyzes eCBs in intact cells and tissue, and that this enzymatic activity controls the efficacy of eCB signaling at cannabinoid receptors. Thus, the results provided by our study suggest that ABHD6 should be added to the list of members of the eCB signaling system.

METHODS

Methods and any associated references are available in the online version of the paper at http://www.nature.com/natureneuroscience/.

Note: Supplementary information is available on the Nature Neuroscience website.

ACKNOWLEDGMENTS

This work was supported by grants from the National Institute on Drug Abuse (DA14486 and DA26430 to N.S., DA017259, DA009789 and DA025285 to B.F.C. and DA026161 to J.L.B.) and from the National Institute of General Medical Sciences (PHS NRSA 2T32 GM007270 to W.R.M.).

AUTHOR CONTRIBUTIONS

W.R.M. prepared the cell cultures, performed the hydrolysis experiments, conducted the data analysis and wrote the manuscript. J.L.B. performed the ABPP experiments and contributed to the data analysis. E.A.H. performed the GC-MS and immunofluoresence experiments and contributed to the electron microscopy experiments and data analysis. A.T. and M.L. performed the electrophysiology experiments. Y.H.L. prepared the cell culture transfections and the shRNA constructs, and performed the qPCR experiments. J.C. contributed to the immunofluorescence experiments. A.L.B. performed the electron microscopy experiments. G.G.M. contributed to the hydrolysis experiments. S.S.-J.H. contributed to antibody production. G.W. and S.F. performed the cell migration experiments. J.P.A. contributed to the ABPP experiments. J.Z.L. and W.L. produced the hydrolase inhibitors. C.X. contributed to the cell culture experiments. T.M. provided the transgenic mice. K.M. provided antibodies. O.J.M. supervised the electrophysiology experiments. B.F.C. supervised the ABPP experiments and the development of hydrolase inhibitors. N.S. supervised the project and wrote the manuscript.

COMPETING FINANCIAL INTERESTS

The authors declare no competing financial interests.

Published online at http://www.nature.com/natureneuroscience/.
Reprints and permissions information is available online at http://www.nature.com/reprintsandpermissions/.

© 2010 Nature America, Inc. All rights reserved.

1. Stella, N. Endocannabinoid signaling in microglial cells. *Neuropharmacology* **56** (Suppl. 1): 244–253 (2009).
2. Horne, E. & Stella, N. The ins and outs of endocannabinoid signaling in healthy and diseased brain. *Future Lipidol.* **3**, 435–452 (2008).
3. Marrs, W. & Stella, N. Measuring endocannabinoid hydrolysis: refining our tools and understanding. *AAPS J.* **11**, 307–311 (2009).
4. Di Marzo, V. Targeting the endocannabinoid system: to enhance or reduce? *Nat. Rev. Drug Discov.* **7**, 438–455 (2008).
5. Katona, I. & Freund, T.F. Endocannabinoid signaling as a synaptic circuit breaker in neurological disease. *Nat. Med.* **14**, 923–930 (2008).
6. Straiker, A. & Mackie, K. Cannabinoids, electrophysiology, and retrograde messengers: challenges for the next 5 years. *AAPS J.* **8**, E272–E276 (2006).
7. Cabral, G.A. & Griffin-Thomas, L. Emerging role of the cannabinoid receptor CB2 in immune regulation: therapeutic prospects for neuroinflammation. *Expert Rev. Mol. Med.* **11**, e3 (2009).
8. Gobbi, G. *et al.* Antidepressant-like activity and modulation of brain monoaminergic transmission by blockade of anandamide hydrolysis. *Proc. Natl. Acad. Sci. USA* **102**, 18620–18625 (2005).
9. Fegley, D. *et al.* Characterization of the fatty acid amide hydrolase inhibitor cyclohexyl carbamic acid 3′-carbamoyl-biphenyl-3-yl ester (URB597): effects on anandamide and oleoylethanolamide deactivation. *J. Pharmacol. Exp. Ther.* **313**, 352–358 (2005).
10. Kathuria, S. *et al.* Modulation of anxiety through blockade of anandamide hydrolysis. *Nat. Med.* **9**, 76–81 (2003).
11. Long, J.Z. *et al.* Selective blockade of 2-arachidonoylglycerol hydrolysis produces cannabinoid behavioral effects. *Nat. Chem. Biol.* **5**, 37–44 (2009).
12. Burston, J.J. *et al.* N-arachidonyl maleimide potentiates the pharmacological and biochemical effects of the endocannabinoid 2-arachidonylglycerol through inhibition of monoacylglycerol lipase. *J. Pharmacol. Exp. Ther.* **327**, 546–553 (2008).
13. Bisogno, T. *et al.* Development of a potent inhibitor of 2-arachidonoylglycerol hydrolysis with antinociceptive activity *in vivo*. *Biochim. Biophys. Acta* **1791**, 53–60 (2009).
14. Long, J.Z. *et al.* Dual blockade of FAAH and MAGL identifies behavioral processes regulated by endocannabinoid crosstalk *in vivo*. *Proc. Natl. Acad. Sci. USA* **106**, 20270–20275 (2009).
15. Blankman, J.L., Simon, G.M. & Cravatt, B.F. A comprehensive profile of brain enzymes that hydrolyze the endocannabinoid 2-arachidonoylglycerol. *Chem. Biol.* **14**, 1347–1356 (2007).
16. Saario, S.M. *et al.* Characterization of the sulfhydryl-sensitive site in the enzyme responsible for hydrolysis of 2-arachidonoyl-glycerol in rat cerebellar membranes. *Chem. Biol.* **12**, 649–656 (2005).
17. Dinh, T.P., Kathuria, S. & Piomelli, D. RNA interference suggests a primary role for monoacylglycerol lipase in the degradation of the endocannabinoid 2-arachidonoylglycerol. *Mol. Pharmacol.* **66**, 1260–1264 (2004).
18. Muccioli, G.G. *et al.* Identification of a novel endocannabinoid-hydrolyzing enzyme expressed by microglial cells. *J. Neurosci.* **27**, 2883–2889 (2007).
19. Jessani, N. *et al.* A streamlined platform for high-content functional proteomics of primary human specimens. *Nat. Methods* **2**, 691–697 (2005).
20. Liu, Y., Patricelli, M.P. & Cravatt, B.F. Activity-based protein profiling: the serine hydrolases. *Proc. Natl. Acad. Sci. USA* **96**, 14694–14699 (1999).
21. Yates, J.R. III, McCormack, A.L. & Eng, J. Mining genomes with MS. *Anal. Chem.* **68**, 534A–540A (1996).
22. Goparaju, S.K., Natsuo, U., Yamaguchi, H. & Yamamoto, S. Anandamide amidohydrolase reacting with 2-arachidonoylglycerol, another cannabinoid receptor ligand. *FEBS Lett.* **422**, 69–73 (1998).
23. Walter, L. *et al.* Non-psychotropic cannabinoid receptors regulate microglial cell migration. *J. Neurosci.* **23**, 1398–1405 (2003).
24. Miller, A.M. & Stella, N. Microglial cell migration stimulated by ATP and C5a involve distinct molecular mechanisms: quantification of migration by a novel near-infrared method. *Glia* **57**, 875–883 (2008).
25. Li, W., Blankman, J.L. & Cravatt, B.F. A functional proteomic strategy to discover inhibitors for uncharacterized hydrolases. *J. Am. Chem. Soc.* **129**, 9594–9595 (2007).
26. Dinh, T.P. *et al.* Brain monoglyceride lipase participating in endocannabinoid inactivation. *Proc. Natl. Acad. Sci. USA* **99**, 10819–10824 (2002).
27. Stella, N. & Piomelli, D. Receptor-dependent formation of endogenous cannabinoids in cortical neurons. *Eur. J. Pharmacol.* **425**, 189–196 (2001).
28. Gulyas, A.I. *et al.* Segregation of two endocannabinoid-hydrolyzing enzymes into pre- and postsynaptic compartments in the rat hippocampus, cerebellum and amygdala. *Eur. J. Neurosci.* **20**, 441–458 (2004).
29. Wilson, R.I. & Nicoll, R.A. Endogenous cannabinoids mediate retrograde signaling at hippocampal synapses. *Nature* **410**, 588–592 (2001).
30. Stella, N., Schweitzer, P. & Piomelli, D. A second endogenous cannabinoid that modulates long-term potentiation. *Nature* **388**, 773–778 (1997).
31. Kano, M., Ohno-Shosaku, T., Hashimotodani, Y., Uchigashima, M. & Watanabe, M. Endocannabinoid-mediated control of synaptic transmission. *Physiol. Rev.* **89**, 309–380 (2009).
32. Lafourcade, M. *et al.* Molecular components and functions of the endocannabinoid system in mouse prefrontal cortex. *PLoS One* **2**, e709 (2007).
33. Maier, S. *et al.* Cellular target genes of Epstein-Barr virus nuclear antigen 2. *J. Virol.* **80**, 9761–9771 (2006).
34. Marrs, W. & Stella, N. 2-AG + 2 new players = forecast for therapeutic advances. *Chem. Biol.* **14**, 1309–1311 (2007).
35. Walter, L., Dinh, T. & Stella, N. ATP induces a rapid and pronounced increase in 2-arachidonoylglycerol production by astrocytes, a response limited by monoacylglycerol lipase. *J. Neurosci.* **24**, 8068–8074 (2004).
36. Witting, A., Walter, L., Wacker, J., Moller, T. & Stella, N. P2X7 receptors control 2-arachidonoylglycerol production by microglial cells. *Proc. Natl. Acad. Sci. USA* **101**, 3214–3219 (2004).

ONLINE METHODS

Drugs. 2-AG was from Cayman Chemical. [^{3}H]-2-AG (radiolabeled on the glycerol moiety) was from American Radiolabeled Chemicals and the National Institute on Drug Abuse drug supply system. WWL70 and JZL184 were synthesized in the laboratory of B. Cravatt. SR144528 was a gift from Sanofi Research.

Cell culture. BV-2 and COS-7 cells were expanded in DMEM (HyClone Cat. # SH30243.01) supplemented with HEPES (10 mM), $NaHCO_3$ (10 mM), penicillin (100 U ml^{-1}), streptomycin (100 μg ml^{-1}) and FBS (10%, HyClone Cat. # SH30071.03). Mouse neurons and microglia in primary culture were prepared as described[23,37] and according to the guidelines of the Institutional Animal Care and Use Committee of the University of Washington. Briefly, for neurons, one day-old mouse brains (C57BL/6) were collected, and their meninges and cerebellum removed. The remaining brain tissue was chopped and the cells dissociated and plated in 10-cm dishes (BD Falcon) coated with poly-D-lysine (0.1 mg ml^{-1}) at 5.0 × 10^5 cells per ml of Neurobasal Medium (Gibco Cat. # 21103-049) supplemented with B-27 (2%), Glutamax (1%), penicillin (100 U ml^{-1}), and streptomycin (100 μg ml^{-1}). Neurons were tested after 7–8 d in culture. For microglia, dissociated cells resulting from two brains were added to DMEM (10 ml) supplemented with $NaHCO_3$ (10 mM), penicillin (100 U ml^{-1}), streptomycin (100 μg ml^{-1}) and FBS (10%), and plated in 75-ml flasks coated with poly-ornithine (0.001%). The resulting floating microglia were plated in uncoated 10-cm dishes at 5.0 × 10^4 cells per ml of MEM (Gibco Cat. # 51200-038) supplemented with CellGro (10%, Cat. # 40-101-CV). Microglia were tested after 24–48 h in culture.

ABPP-MudPIT analysis of BV-2 cytosolic and mitochondrial proteomes. BV-2 cells in culture were detached, rinsed by centrifugation, resuspended in Tris buffer (300 μl, 50 mM, pH 7.5) and lysed by sonication. Cytosolic and mitochondrial fractions were prepared as described[18], and shipped to the Cravatt laboratory for ABPP-MudPIT analysis. Specifically, BV-2 cytosolic and mitochondrial proteomes (1 mg in 1 ml Tris buffer) were incubated with FP-biotin (5 μM, 1 h, room temperature). Enrichment of the FP-labeled proteome was performed as described[19], except that the Lys-C digestion step was omitted. MudPIT analysis was performed as described on an LTQ ion trap mass spectrometer (ThermoFisher) coupled to an Agilent 1100 series HPLC[19]. The tandem MS data were searched against the mouse IPI database with the SEQUEST algorithm, and results were filtered and grouped with DATASELECT[38]. Peptides with cross-correlation scores greater than 1.8 (+1), 2.5 (+2), 3.5 (+3) and δCN scores >0.08 were included in subsequent spectral counting analysis. The average spectral counts of two cytosolic and three mitochondrial samples are reported for serine hydrolases with average spectral counts >15 and greater than tenfold enrichment in mitochondrial versus cytosolic samples.

qPCR. RNA was extracted using PerfectPure RNA Cultured Cell Kit (5 Prime). Reaction mixtures were prepared using Brilliant II 1-Step QRT-PCR Master Mix (Stratagene). Primer and probe combinations were designed using the Roche Universal Probe Library Assay Design Center (http://www.universalprobelibrary.com). Primers were from Operon and universal probes were from Roche. Reactions were run using a Stratagene Mx3000P QPCR system and consisted of 30 min incubation at 45 °C, followed by a 10-min denaturation at 95 °C and 40 cycles of 1 min at 95 °C and 30 s at 60 °C.

shRNA. Plasmids expressing shRNAs were purchased from the Sigma MISSION shRNA library or constructed in our laboratory (targeting sequences were inserted into pLKO.1 (Addgene plasmid 10878), according to the manufacturer's instructions[39]). Each set of plasmid carrying a specific shRNA construct was transfected into AD293 cells using Lipofectamine 2000 (Invitrogen, according to the manufacturer's instructions). After 72 h, the supernatant of AD293 containing the lentiviruses was applied directly to BV-2 cells. After 16 h, the medium of BV-2 cells was replaced by DMEM supplemented with FBS (10%). After 24 h, the medium of BV-2 cells was replaced by DMEM supplemented with FBS (10%) and puromycin (2 μg ml^{-1}), and cells were kept for 5–9 d in culture for selection. qPCR was systematically performed on each batch to assess for % knockdown. Selected clones were then split and expanded for specific experiments.

Cell migration. Cell migration was performed and calculated as described[24]. Briefly, BV-2 cells were incubated for 30 min in MEM containing the nuclear fluorescent dye DRAQ5. Cells were then resuspended in MEM supplemented with Cellgro (10%) and loaded in upper chamber of a 96-well chemotaxis apparatus (Neuroprobe, 7 × 10^4 cells per 390 μl, filters with 10-μm pores). Lower wells contained the same medium supplemented with 2-AG. Migration occurred over 3 h (37 °C, 5% CO_2), after which the filter was removed and the cells that had not migrated were thoroughly wiped off the top side of the filter. The fluorescence emitted by the cells that had migrated toward the bottom surface of the filter was measured using an Odyssey Infrared Imaging System (LI-COR).

Transfections. COS-7 cells (~90% confluent in 10-cm dishes) were transfected with expression vectors (OpenBioSystems, 3 μg per dish) by using Lipofectamine 2000. After 4–6 h, the medium was changed and the cells were incubated for an additional 30–36 h in DMEM + FBS (10%). For ICC, transfections were performed similarly, but using cells grown on 12-mm coverslips placed in 24-well plates (~60% confluent). Here, GFP-expressing vectors (40 ng) were also added to identify the cells that had been transfected.

[^{3}H]-2-AG hydrolysis in cell homogenates and intact cells. Cell homogenates were prepared as described[18]. Homogenates were added to silanized glass tubes that contained 100 μl of Tris-HCl buffer (100 mM, pH 7.4) supplemented with fatty acid-free BSA (0.1%), [^{3}H]-2-AG (~1 nM) and inhibitors or vehicle (DMSO, 0.1%). Tubes containing this solution, but without cell homogenate, were used as control for non-enzymatic [^{3}H]-2-AG hydrolysis (blank) and this value was systematically subtracted from values obtained with homogenates. Tubes were incubated for 10 min in a shaking water bath at 37 °C. Reactions were stopped by adding ice-cold MeOH-$CHCl_3$ (1:1, 2 ml) and vortexing. Linear enzymatic activity with a set amount of protein was systematically verified and chosen for each homogenate. The hydrophobic and hydrophilic phases were separated by centrifugation (800*g*, 10 min). One milliliter of upper phase was recovered and mixed with Ecoscint (4 ml) for radioactivity determination by liquid scintillation. For intact cells, the following '[^{3}H]-2-AG solution' was prepared in a silanized glass vial and allowed to equilibrate at room temperature for 75 min: MEM supplemented with BSA (0.15%) and [^{3}H]-2-AG (~1 nM). Cells grown in 12-well plates were pre-treated with inhibitors or vehicle for 30 min by adding 0.1 ml to each well. Cells were then rinsed twice with MEM supplemented with fatty acid-free BSA (0.15%) and incubated with [^{3}H]-2-AG solution for 20 min (with gentle shaking in a water bath at 37 °C). Non-specific hydrolysis was determined by adding 2-AG (100 μM), and this value was systematically subtracted from each data point. The entire medium (~1 ml) was recovered in a silanized glass tube, ice-cold MeOH (2 × 1 ml) was added to the cells, and the resulting lysate pooled with the media. $CHCl_3$ was added such that there was a final ratio of 1:2:2 for MEM:MeOH:$CHCl_3$. The amount of [^{3}H]-glycerol present in the hydrophilic phase was quantified by liquid scintillation as described above.

ICC and IHC. The following primary and secondary antibodies were used: affinity-purified ABHD6 (rabbit polyclonal, 1:2000 (IHC), 1:10,000 (ICC)), CB1 (guinea pig polyclonal, raised against the full carboxyl terminus of rat CB1, 1:2,000 (ICC and IHC)[40]), MAP2 (mouse monoclonal, 1:500, Chemicon), SMI32 (mouse monoclonal, 1:1,000, AbCAM), GFAP (mouse monoclonal, 1:400, Millipore), GFP (mouse monoclonal, 1:400, Invitrogen), goat anti-rabbit conjugated with Texas Red (1:250, Invitrogen) or conjugated with Alexa555 for triple staining experiments (1:500, Invitrogen), goat anti-guinea pig conjugated with Alexa488 (1:500, Invitrogen), goat anti-mouse conjugated with Alexa647 (1:500, Invitrogen). Antibodies were diluted in PBS supplemented with donkey serum (2.5%) and Triton X-100 (0.5%) with or without 5 μg ml^{-1} of the immunizing peptide and shaken at 4 °C for 18 h. For ICC, cells were fixed with PFA (4% in PBS) for 20 min (warming from 4 °C to room temperature), permeablized with PBS supplemented with goat serum (5%) and saponin (0.1%) at room temperature for 30 min, incubated for 18 h at 4 °C in PBS supplemented with goat serum (2.5%), and incubated in PBS supplemented with Fc block (0.5 μg per cover slip; BD Bioscience) for 5 min at room temperature. Cells were then incubated with primary antibodies for 90 min at room temperature, washed 5× with PBS at room temperature and incubated for 1 h at room temperature with secondary antibodies. Cells were then rinsed 7× in PBS and once with de-ionized water. Cover slips were mounted with Vectashield and sealed with nail polish. For IHC, mice (WT C57BL/6, GAD67-GFP C57BL/6 or Iba1-GFP C57BL/6; 8 wks old) were perfused and fixed with PFA (4% in PBS), and whole brains cryoprotected in 15%

© 2010 Nature America, Inc. All rights reserved.

doi:10.1038/nn.2601

sucrose (24 h), followed by 30% sucrose (48 h). Coronal sections that included the prefrontal cortex (30 μm) were prepared using a microtome and stored in PBS at 4 °C. Sections were rinsed 3× with PBS and incubated for 90 min at room temperature with PBS supplemented with donkey serum (5%) and Triton X-100 (1%). Primary antibodies, which had been incubated for 16–18 h with or without 5 μg ml^{-1} of the inoculation peptide in PBS supplemented with donkey serum (2.5%) and Triton X-100 (0.5%), were applied to each section for 16–18 h at 4 °C with gentle agitation. Sections were then rinsed 6× with PBS supplemented with Tween-20 (0.05%, at room temperature). Sections were then incubated with secondary antibodies diluted in PBS with supplemented with donkey serum (2.5%) and Triton X-100 (0.5%) for 1 h at room temperature with gentle agitation, followed by seven rinses with PBS and one rinse with deionized water. Sections were mounted onto charged slides and allowed to dry for ~18 h, after which coverslips were mounted with Vectashield and sealed with nail polish. All fluorescent images were collected on a Zeiss Axio Observer Z1 equipped with a Pan-Apochromatic 20×/0.8DicII (single plane) or Pan-Apochromatic 63×/1.4 oil lens (Z-stack images at 0.26 μm that were deconvolved using an Apotome). The same exposure settings were used for the experimental, immunizing peptide, and secondary only controls. Images were processed in Photoshop by gating the background to the secondary-only control. The intensity was gated to the experimental image and was the same setting used for the immuninizing peptide control.

Electron microscopy. Two C57BL/6 mice were perfused by one of two methods (similar results were obtained independent of the perfusion method). Both mice were perfused through the heart by first washing with saline followed by either (i) 4% paraformaldehyde with 0.1% glutaraldehyde (TAAB) in acetate buffer (pH 6.0; 5 min) followed by 4% paraformaldehyde with 0.1% glutaraldehyde in borate buffer (pH 8.5; 50 min)[41]; or (ii) 4% paraformaldehyde with 0.1% glutaraldehyde for 30 min. Immediately after perfusion, the brain of each mouse was dissected and coronal sections (50 μm) were cut using a vibratome. All incubations and washes were carried out on a horizontal shaker. The sections were washed in phosphate buffer (PB: 5×; 10 min) and incubated in 30% sucrose in PB overnight at 4 °C. Slices were freeze-thawed over liquid nitrogen three times to ensure penetration and then washed in PB (3×; 10min) before being treated with 0.5% sodium borohydride in PB (15 min). After washes in PB (3×; 10 min) the slices were transferred to 0.05 M Tris-buffered saline (TBS; pH 7.4) before being blocked for 40 min in BSA (3%) in TBS at room temperature. ABHD6 polyclonal antibody (1:1,500, rabbit) was diluted in TBS and incubated with the slices overnight at room temperature. After 18 h, the slices were washed with TBS (4×; 10 min) before being incubated with ultra small gold-conjugated rabbit secondary (1:50; Aurion) diluted in TBS with 0.8% BSA, 0.1% gelatin and 0.05% sodium azide overnight at 4 °C. After washes in the same solution (1×; 30 min) and TBS (3×; 10min) the slices were postfixed with 2% glutaraldehyde and silver intensified with Aurion R-Gent intensification kit for 15 min.

After intensification, sections were dehydrated by treating with OsO_4 (1% for 1 min then 0.5% for 20 min on ice water), then dehydrated in ethanol and propylene oxide and finally embedded in Durcupan (Fluka). During the 70% ethanol step, the sections were treated with 1% uranyl acetate in 70% ethanol for 40 min. Selected blocks containing different cortical areas within layer 4–5 were selected to be cut into 60-nm ultrathin sections with an Ultramicrotome (Reichert) and mounted on copper grids. Contrast staining was then done with lead citrate for 3 min.

We collected 60,000× magnified images using a camera (Morada; Olympus) mounted to an electron microscope (JEM 1200 EXII; Jeol). Specifically, synaptic contacts (which had both an obvious postsynaptic density within a reasonably small postsynaptic site and vesicle accumulation in the presynaptic site, as well as a synaptic gap between the two sites) containing at least 1 gold particle on either the pre- or postsynaptic side were collected for analysis. Images were analyzed using ImageJ software (NIH) by manually counting gold particles within both pre- and postsynaptic elements of previously specified synapses, and the area of each element was also measured. The number of gold particles was normalized to the area of each element for comparison.

eCB levels. Cells grown in 10-cm dishes (one dish per condition) were pretreated for 30 min with inhibitors or vehicle (DMSO, 0.1%) by adding 1 ml directly to the medium (37 °C, shaking water bath). To stimulate the neurons, glutamate (100 μM) and carbachol (1 mM) were added in 1 ml for an additional 2.5 min[27]. The reaction was stopped by collecting the medium and adding 5 ml of ice-cold methanol. 2-AG and anandamide were extracted, purified and their levels determined as described[42]. Briefly, the cell medium and homogenate were added to $CHCl_3$ containing d_5-2-AG (150 pmol) and d_4-anandamide (50 pmol) for Folch extraction. The organic phase was recovered and dried under N_2, and anandamide and 2-AG partially purified by solid-phase chromatography columns (silica), eluting them with ethylacetate/acetone (1:1, 2 ml). The eluate was then dried under N_2, derivitized with BSTFA (SupelCo) and analyzed by CI-GC-MS (Varian CP-8400 Autosampler, CP3800 Varian GC, Varian Saturn 2000 mass spectrometer).

Electrophysiology. Electrophysiology experiments were performed in Bordeaux, France according to the criteria of the European Communities Council Directive (86/609/EEC) and the United States National Institutes of Health *Guide for the Care and Use of Laboratory Animals*. Mouse brain slices (C57BL/6, ~8 wks old, 300 μm) were prepared as described[32]. In brief, immediately after cutting, slices containing the prefrontal cortex were stored for ~30 min at 32–35 °C in artificial cerebrospinal fluid (ACSF) containing (in mM): NaCl (126), KCl (2.5), $MgCl_2$ (2.4), $CaCl_2$ (1.2), $NaHCO_3$ (18), NaH_2PO_4 (1.2) and glucose (11), and equilibrated with 95% O_2/5% CO_2. Slices were then placed in the recording chamber at room temperature and superfused with ACSF (2 ml min^{-1}, 32–35 °C). The superfusion medium contained picrotoxin (100 μM) to block $GABA_A$ receptors. Inhibitors were added at the final concentration to the superfusion medium. To evoke synaptic currents, stimuli (100–150 μs duration) were delivered at 0.1 Hz through a glass electrode filled with ACSF placed in layer 2/3. The recording pipette was placed in layer 5/6 and was also filled with ACSF. Both the field excitatory postsynaptic potential (fEPSP) area and amplitude were measured (graphs depict area).

Data analysis. Values are expressed as mean ± s.e.m. Statistical analysis and dose-response curves were generated using GraphPad PRISM (version 4).

37. Stella, N., Pellerin, L. & Magistretti, P. Modulation of the glutamate-evoked release of arachidonic acid from mouse cortical neurons: involvement of a pH-sensitive membrane phospholipase A2. *J. Neurosci.* **15**, 3307–3317 (1995).
38. Eng, J., McCormack, A.L. & Yates, J.R. III. An approach to correlate MS/MS data to amino acid sequence in a protein database. *J. Am. Soc. Mass Spectrom.* **5**, 976–989 (1994).
39. Moffat, J. *et al.* A lentiviral RNAi library for human and mouse genes applied to an arrayed viral high-content screen. *Cell* **124**, 1283–1298 (2006).
40. Berghuis, P. *et al.* Hardwiring the brain: endocannabinoids shape neuronal connectivity. *Science* **316**, 1212–1216 (2007).
41. Berod, A., Hartman, B.K. & Pujol, J.F. Importance of fixation in immunohistochemistry: use of formaldehyde solutions at variable pH for the localization of tyrosine hydroxylase. *J. Histochem. Cytochem.* **29**, 844–850 (1981).
42. Muccioli, G.G. & Stella, N. An optimized GC-MS method detects nanomolar amounts of anandamide in mouse brain. *Anal. Biochem.* **373**, 220–228 (2007).

© 2010 Nature America, Inc. All rights reserved.